Proceedings of the 9th World Congress on Mechanical, Chemical, and Material Engineering (MCM'23)
Brunel University, London, United Kingdom - August 06-08, 2023
Paper No. ICMIE 137
DOI: 10.11159/icmie23.137

3D Printed Structures for Under Water Robots Design

Jose Luis Ordoñez-Avila[1], Silvio Javier Lazaro-Cardenas[2], Rodrigo Espinal Lanza[2]
FI, Universidad Tecnológica Centroamericana (UNITEC)
San Pedro Sula, Cortés, Honduras
jlordonez@unitec.edu, silviolazaro@unitec.edu, rodriespinal@gmail.com

Abstract **-** Nowadays, with the continuous development of low-cost technologies such as 3D printing and open source hardware and software, the cost of building an ROV has been further reduced. This is why the present research aims to analyse the calculations necessary for the development of an ROV prior to its construction, obtaining significant improvements in design as well as a reduction of time and costs. This paper shows a comparison of the design parameters of a 3 DOF robot with 4 turbines and a 5 DOF robot with 6 turbines, to demonstrate the importance of CAD and CFD in underwater robots' design. The selection of actuators is based on the results of CFD, obtaining linear and quadratic, turbine rpm and the friction coefficient to determine the stability of the robot. A reduction in time and costs was obtained through CFD analysis prior to robot construction. The comparison between the open and close structures is evident that the close structure design in this paper has more stability and is better option for underwater robots. 3D printing is a good alternative for underwater robots, the infill should be 100% to avoid leaks and breaks based on the stress test. The mayor disadvantage of 3D printing is the manufacturing time.

Keywords**:** CAD, CFD, 3D printing, DOF, PRBS

1. Introduction

It The development of underwater robots has revolutionized many industries due to its numerous applications in the offshore oil and gas industry, the defence sector, search and rescue, oceanographic research, and environmental monitoring [1]. Over the years, researchers have focused on designing underwater robots that can adapt to different environments and perform various tasks. For example, [2] made a modular underwater robot that could self-reconfigure by stacking and unstacking its component modules, which was used for monitoring and exploration, [3] designed an underwater robot using an Arduino based platform and handmade waterproof thrusters controlled by an android smartphone.

In recent years, advancements in 3D printing technology have enabled researchers to manufacture underwater robots with complex geometries and intricate details using CAD designs, which in [4] review, there have been various uses such as sample collection, hydrodynamics, and coral reef restoration. For instance, [5] designed their underwater robot using 3D printing and a Xilinx Zyng-700 module. This technology has made it possible to create customizable robots that can perform specific tasks in underwater environments, while also reducing production costs. Additionally, as highlighted by [6], underwater robots can also be used for monitoring nuclear power plants. Sensors are an essential component of underwater robots that enable them to navigate, locate objects, and gather data. For example, [7] designed a robotic detection system based on the fish's lateral line to monitor underwater environments. Such sensors help robots operate effectively in low visibility and underwater conditions according to [8]. The aim of this paper is to demonstrate the use of CAD and CFD for under water robots design by using 3D printing.

2. Method

The design of submersible robots has a degree of complexity and costs, so the use of CAD/CFD allows to reduce costs and estimate robot improvements. In this work we rely on the methodology proposed [9] which uses CAD/CFD design to obtain design parameters for submersible robots. A comparison of the design parameters of a 3 DOF robot with 4 turbines and a 5 DOF robot with 6 turbines is shown. Ensuring the operation of such a sophisticated machine is always a great challenge, so the project has been developed using high-level engineering software such as solidworks where it was possible to preliminarily design how the robots behave if they move.

3. Results

3.1. CAD Design

The CAD design of the 3 DOF robot consists of a 3" diameter waterproof capsule, a shell printed in PEEK and stainless steel clamps to join both parts. This robot has an open structure leaving the fluid pass inside the structure. The second robot structure consists of a plastic shell, printed in PEEK at a rate of 100% infill between printing layers, sealed with epoxy resin to seal any type of opening between the filaments. A layer of Carbon Fiber is added to increase its mechanical properties and resistance to water pressure making a close structure. It contains an airtight tube where all its electronic components are stored Table 2 shows the CAD parameters of both robots.

Table 2: CAD parameters of both robots.

Parameter	Symbol	Unit	Robot 1	Robot 2
Mass	m	kg	5.803	8.409
Buoyancy	B	N	64.67	82.03
Weight	W	N	56.92743	82.49
Inertia	Ix	$Kg \cdot m^2$	0.06669207	0.121619
	Iy		0.08182423	0.217961
	Iz		0.131617	0.302178
	lxx		0.08182375	0.217961
	lyx		-8.51E-05	-5.951E-05
	lzx		8.53E-06	2.572E-05
	lxy		-8.51E-05	-5.947E-05
	lyy		0.06672717	0.302051
	lzy		0.001498977	0.0006786
	lxz		8.53E-06	2.572E-05
	Iyz		0.000149897	0.0006786
	lzz		0.000131582	0.12156
Volume	v	m^3	0.0045521	0.0081611
Large	L	mm	347	510
Width	a	mm	400	470
Height	h	mm	164.64	240

3.2. Stress test

The stress tests were performed starting at 10 meters depth, reaching minimum deformations and with a safety factor greater than 3. In a second test, the stress study was performed at 25 meters depth as shown in Figure 1, reaching a minimum mechanical displacement for robot 1 and the lower displacement in robot 2. The safety factor (FOS) for

robot 1 at 25 meters depth was just greater than 1 and robot 2 has a FOS greater than 4. The close structure is more resistant than the open structure due to its geometry and mass.

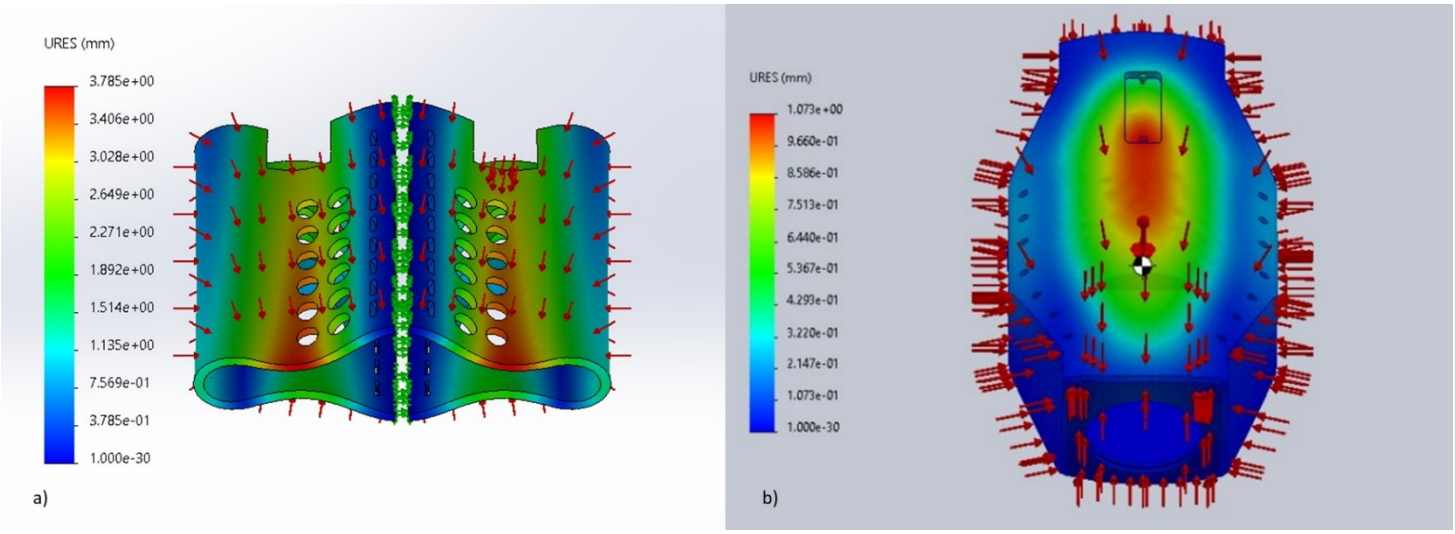

Fig. 1: a) Stress test for the open structure; b) Stress test for the close structure.

3.3. Computer Fluid Dynamics (CFD)

Velocity tests are performed using CFD to determine the polynomial regressions based on simulations. These equations are used to develop the dynamic models of the robot. Vorticity and flow direction tests are performed on the ROV in order to identify the hydrodynamics exerted on it. These tests show the hydrodynamic flows that are generated as the robot moves forward. Figure 2 analyses the hydrodynamics of the fluid now of impact with both robots. In the case of the open structure robot, a greater displacement of the water is observed than in the closed structure, generating a greater number of vortices inside the structure. These vortices are generated by the impact of the hydrodynamic fluid on the vertical turbines at a velocity of approximately 0.207 m/s. On the other hand, the closed structure robot only generates vortices when the hydrodynamic fluid passes through the vertically positioned turbines. Figure 3 shows the spheres in which the fluid behaves while the robot advances at 2.5 m/s, in the open structure the spheres moves down the robot creating more disturbance than in the close structure.

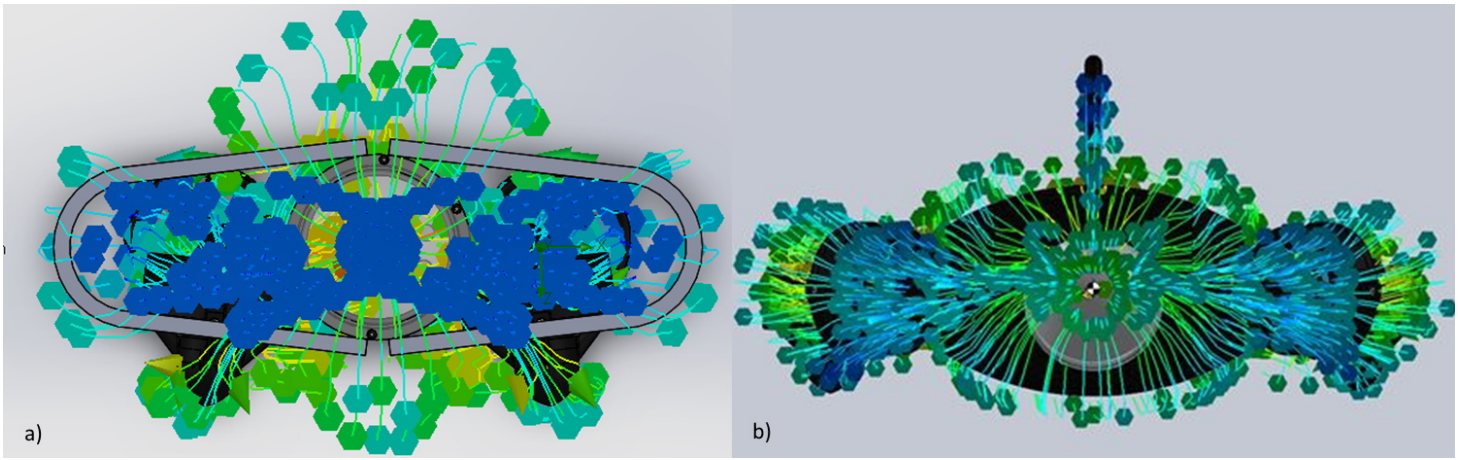

Fig. 2: a) Frontal CFD test for the open structure; b) Frontal CFD test test for the close structure.

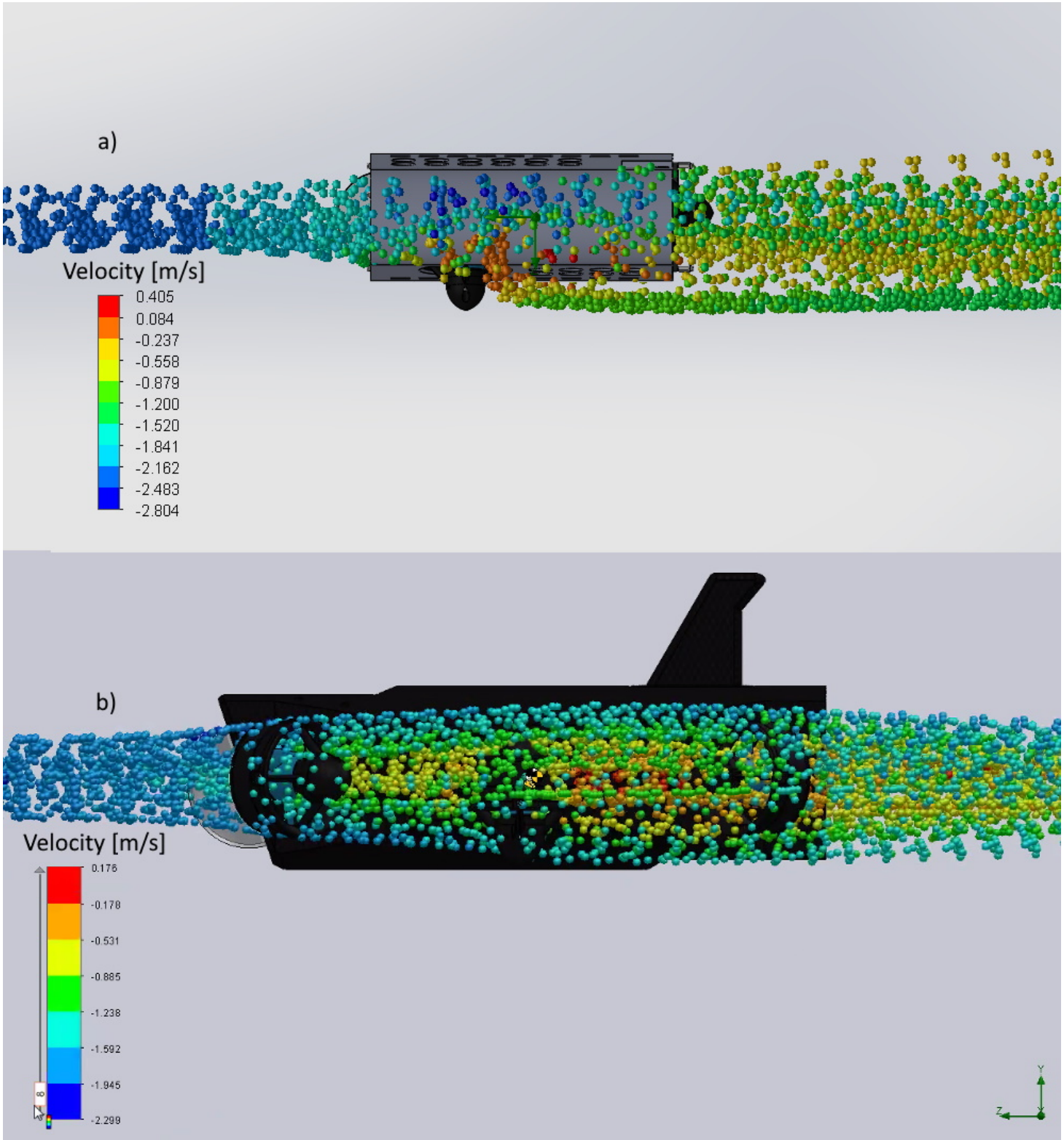

Fig. 3: a) Lateral CFD test for the open structure; b) Lateral CFD test for the close structure.

The results of the simulation can be found in Table 3, the dynamic pressure exerted by the fluid in the open-structured structured robot was higher than that of the closed structure, generated mostly by the vortices observed in the simulation. This pressure in both cases is lower than that of the stress test that was performed so the robot structures can withstand the the pressure. Regarding the fluid density and velocities both robots obtained the same behaviour since they are input parameters of the simulation. The force necessary for the robot to move at 2.5 m/s in this fluid is given by the force on the the Z-axis, while the vortices and disturbances create forces on the Y-axis. The friction forces and torques in both cases are low since the simulation is only performed on one axis. For this it is necessary to make a simple system with the hydrodynamics of the robot, on the other hand the hydrostatics is what allows an object to float or sink, so for the robot zero buoyancy is needed to avoid excessive use of the turbines.

Table 3: CFD Comparison data results of 2.5 m/s

		Robot 1			Robot 2		
Goal Name	Unit	Average	Min	Max	Average	Min	Max
GG Maximum Dynamic Pressure 1	[Pa]	4283.0	4227.6	4329.4	3027.4	3027.3	3027.5
GG Average Density (Fluid) 2	[kg/m^3]	997.6	997.6	997.6	997.6	997.6	997.6
GG Average Velocity 3	[m/s]	2.5	2.5	2.5	2.5	2.5	2.5
GG Average Velocity (X) 4	[m/s]	0.0	0.0	0.0	0.0	0.0	0.0
GG Average Velocity (Y) 5	[m/s]	0.0	0.0	0.0	0.0	0.0	0.0
GG Average Velocity (Z) 6	[m/s]	-2.5	-2.5	-2.5	-2.5	-2.5	-2.5
GG Force 7	[N]	91.6	91.5	91.7	77.2	77.0	77.4
GG Force (X) 8	[N]	-0.8	-1.0	-0.7	-1.0	-1.1	-0.9
GG Force (Y) 9	[N]	6.7	6.6	6.9	3.8	3.7	4.0
GG Force (Z) 10	[N]	-91.4	-91.5	-91.3	-77.1	-77.3	-76.9
GG Normal Force 11	[N]	88.5	88.4	88.9	74.64	74.52	74.80
GG Friction Force 12	[N]	3.72	3.65	3.84	2.57	2.45	2.73
GG Friction Force (X) 13	[N]	0.0	0.0	0.0	0.0	0.0	0.0
GG Friction Force (Y) 14	[N]	-0.1	-0.1	-0.1	0.0	0.0	0.0
GG Friction Force (Z) 15	[N]	-3.5	-3.5	-3.5	-2.6	-2.7	-2.5
GG Torque (X) 16	[N*m]	1.8	1.8	1.8	-24.3	-24.4	-24.3
GG Torque (Y) 17	[N*m]	9.1	9.1	9.1	12.9	12.9	13.0
GG Torque (Z) 18	[N*m]	0.6	0.6	0.6	1.2	1.2	1.2

Finally, the selection of actuators is based on the results obtained. An example of this is the obtaining of linear and quadratic coefficients in a robot in (1) and (2) based on the data obtained in Figure 4. These are achieved by performing several simulations by changing the fluid velocity and plotting the average force and torques as a dependent variable of a polynomial regression given by the velocity. It is also possible to calculate the turbine rpm by applying (2) based on [10]. Even the determination of the friction coefficient can determine the stability of the robot [11].

$$f_{rz} = -9.9469\, {v_z}^2 - 7.7966\, v_z + 3.9084 \qquad (1)$$

$$\tau_z = 0.7927\, {\omega_z}^2 - 0.1068\, \omega_z + 0.0581 \qquad (2)$$

$$\omega = -2.315f^2 + 149.75f + 52.15 \quad (3)$$

$$\mu = \frac{f_r}{f_n} \quad (4)$$

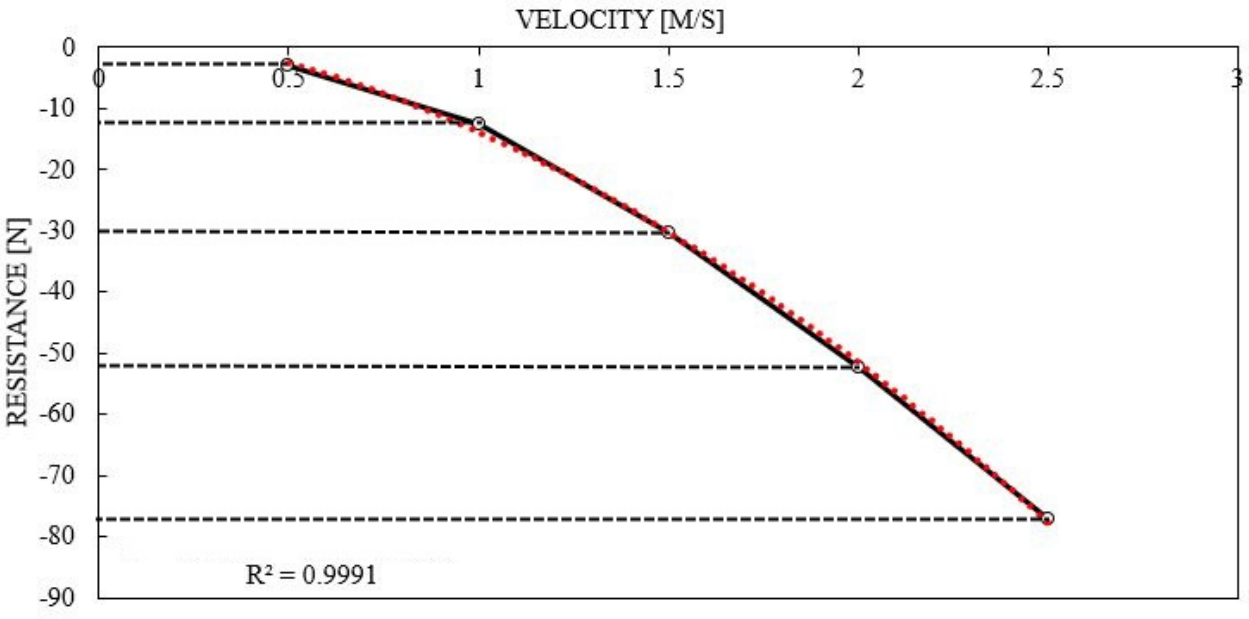

Fig. 4: Polynomial regression based on simulation (PRBS) for robot 2.

3.4. 3D printing fabrication

For the manufacture of a 3D printed robot it is necessary to take into account the material with which the printing is going to be done. In the case of both robots, we chose to make the impression in PEEK material, is also known as polyether ether ketone, this is a high-quality material and excellent mechanical properties, thanks to its strength and hardness in environments with high requirements. When performing a 3D printing we have to take into account the printer with which the printing process will be performed, in this case we used an ender cr-10 max for its ability to print large parts, we must also take into account the time it will take to perform the prints, for the case of robot 1 two pieces were made while robot 2 was performed by 12 prints, their values are shown in Table 4. When performing 3D printing should be performed with a filling of 100%, this to avoid breaks between the filament and have a better performance at high depths. Robot 2 was printed with 100% infill because it is a closed design and with its electronic components inside, it had to be well protected.

Table 4: 3D printing comparison between an open and closed structure

	Robot 1	Robot 2
Parts	2	12
Mass	3054	3026
Time	106	91
Infill	100%	100%

4. Conclusion

The method used for the manufacture of under water robots was validated, obtaining a notable improvement in the CAD CAD designs as well as in the final product. A reduction in time and costs was obtained through CFD analysis prior to robot robot construction. The comparison between the open and close structures is evident that the close structure design in this this paper has more stability and is better option for underwater robots as shown in Figure 5. 3D printing is a good alternative for underwater robots, the infill should be 100% to avoid leaks and breaks based on the stress test. The mayor disadvantage of 3D printing is the manufacturing time. Thanks to the CAD and CFD calculations we were able to observe small differences between an open and a closed design, considering its structural design, a similar printing time and amount of material used to make them. It was also observed that in this case the open design with a lot of space for water flow can be more affected than a closed structure.

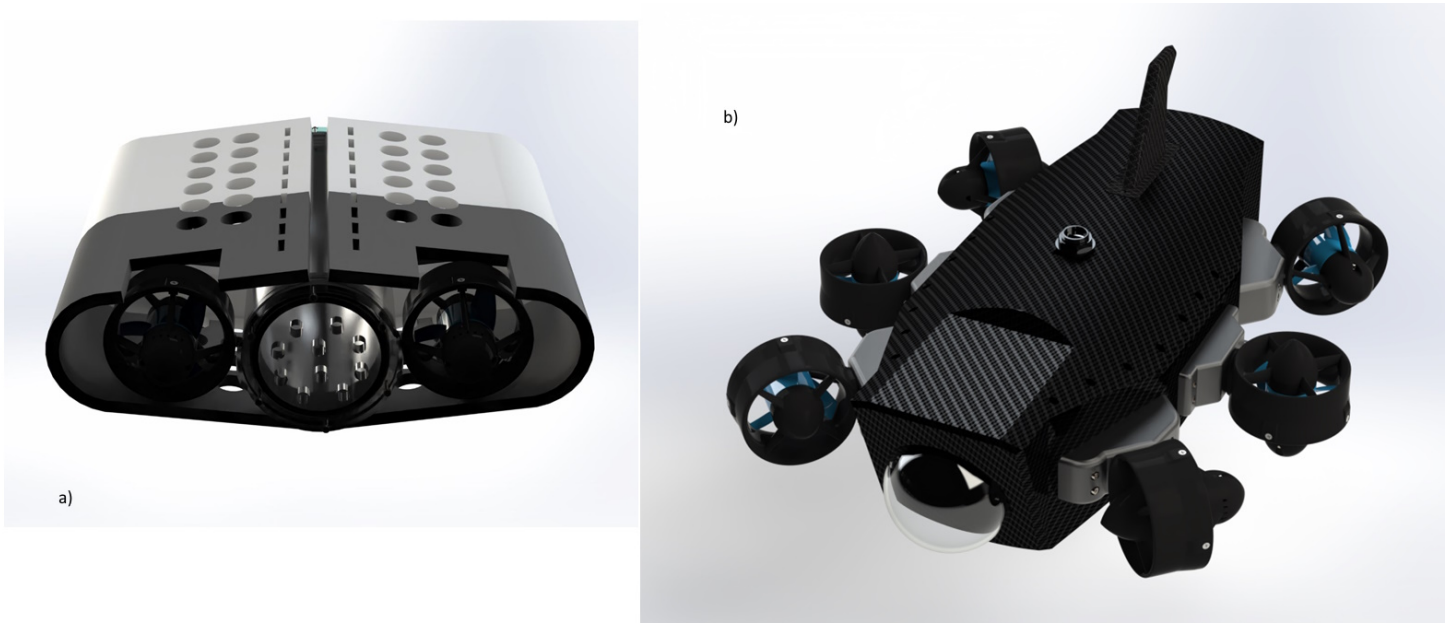

Fig. 5: a) Robot 1: Open structure render; b) Robot 2: Close structure render.

References

[1] R. Bogue, “Underwater robots: a review of technologies and applications”, Ind. Robot Int. J., vol. 42, núm. 3, pp. 186–191, ene. 2015, doi: 10.1108/IR-01-2015-0010.

[2] I. Vasilescu, P. Varshavskaya, K. Kotay, y D. Rus, “Autonomous Modular Optical Underwater Robot (AMOUR) Design, Prototype and Feasibility Study”, en Proceedings of the 2005 IEEE International Conference on Robotics and Automation, abr. 2005, pp. 1603–1609. doi: 10.1109/ROBOT.2005.1570343.

[3] S. K. Deb, J. H. Rokky, T. C. Mallick, y J. Shetara, “Design and construction of an underwater robot”, en 2017 4th International Conference on Advances in Electrical Engineering (ICAEE), sep. 2017, pp. 281–284. doi: 10.1109/ICAEE.2017.8255367.

[4] J. S. Mohammed, “Applications of 3D printing technologies in oceanography”, Methods Oceanogr., vol. 17, pp. 97–117, dic. 2016, doi: 10.1016/j.mio.2016.08.001.

[5] S. Pan, S. Guo, L. Shi, Y. He, Z. Wang, y Q. Huang, “A spherical robot based on all programmable SoC and 3-D printing”, en 2014 IEEE International Conference on Mechatronics and Automation, ago. 2014, pp. 150–155. doi: 10.1109/ICMA.2014.6885687.
[6] A. Mazumdar, M. Lozano, A. Fittery, y H. Harry Asada, “A compact, maneuverable, underwater robot for direct inspection of nuclear power piping systems”, en 2012 IEEE International Conference on Robotics and Automation, may 2012, pp. 2818–2823. doi: 10.1109/ICRA.2012.6224619.
[7] Z. Tang, Z. Wang, J. Lu, G. Ma, y P. Zhang, “Underwater Robot Detection System Based on Fish’s Lateral Line”, Electronics, vol. 8, núm. 5, Art. núm. 5, may 2019, doi: 10.3390/electronics8050566.
[8] Y. Cong, C. Gu, T. Zhang, y Y. Gao, “Underwater robot sensing technology: A survey”, Fundam. Res., vol. 1, núm. 3, pp. 337–345, may 2021, doi: 10.1016/j.fmre.2021.03.002.
[9] M. C. Paredes-Sanchez, D. A. Jimenez-Nixon and J. L. Ordoñez-Avila, "Underwater Robot Design Proposed Method Based on CAD and CFD," 2022 IEEE Central America and Panama Student Conference (CONESCAPAN), San Salvador, El Salvador, 2022, pp. 1-6, doi: 10.1109/CONESCAPAN56456.2022.9959715.
[10] J. L. O. Avila, M. G. O. Avila and M. E. Perdomo, "Design of an Underwater Robot for Coral Reef Monitoring in Honduras," 2021 6th International Conference on Control and Robotics Engineering (ICCRE), Beijing, China, 2021, pp. 86-90, doi: 10.1109/ICCRE51898.2021.9435710.
[11] Christ, Robert D., and Robert L. Wernli. 2007. The ROV Manual: A User Guide to Observation-Class Remotely Operated Vehicles. 1st ed. Amsterdam ; Boston: Butterworth-Heinemann.